

## TOWARDS THE LAMBERTIAN LIMIT IN THIN FILM SILICON SOLAR CELLS WITH PHOTONIC STRUCTURES

L.C. Andreani, A. Bozzola, P. Kowalczewski, and M. Liscidini  
 Dipartimento di Fisica, Università degli Studi di Pavia  
 Via Bassi 6, 27100, Pavia - Italy

**ABSTRACT:** We theoretically investigate light trapping in thin film crystalline silicon solar cells with ordered and disordered photonic structures using the Rigorous Coupled Wave Analysis formalism. The general aspects of these two complementary optical designs are presented, focusing on the absorption in the active material and on the resulting photo generated current, which are assumed as the figures of merit. A comparison with the Lambertian limit to light trapping for the 1D and 2D cases is performed. We show that the diffraction of light and the improved impedance matching are responsible for the increased efficiency of the photonic devices. These effects are first investigated in ordered 1D and 2D photonic patterns and in 1D rough scattering surfaces, which are assumed as prototypes for pure ordered and disordered systems. We then propose a final design consisting of a 1D lattice with engineered size and position disorder to take advantage of both the approaches. The resulting structures show a broad band absorption enhancement, which results in higher photocurrent and it is very close to the 1D Lambertian limit. These results point out that an engineered combination of order and disorder is the optimal solution in terms of optical design.

**Keywords:** Light trapping, c-Si, thin film solar cell

### 1 INTRODUCTION AND NUMERICAL METHOD

The trapping of solar light into active semiconductor materials is gaining large interest in order to find a way to increase the absorption in thin film solar cells, while keeping reasonable conversion efficiency and reducing the manufacturing costs [1-5]. Recent progresses in epitaxy-free growth techniques and nano imprinting methods show that it is possible to produce few microns thick crystalline Silicon (c-Si) solar cells [11] and then to pattern them using potentially large scale methods [12]. In this paper we investigate the light trapping properties of different types of ordered and disordered photonic structures integrated in a realistic c-Si solar cell architecture. The optical properties of the devices are calculated using the Rigorous Coupled Wave Analysis formalism [13,14]. For the modelling of disordered structures, a super cell framework is introduced. The main input parameters of our numerical method are the vertical stack of the cell and the in-plane Fourier transform of the periodic dielectric function. All the energy-dependent dielectric functions of the involved materials are taken from Ref. [15]. The number of plane waves is chosen to ensure the convergence of the result in the energy window which is more useful for photovoltaics (from the c-Si band gap up to 3.5 eV). Typically around 200 plane waves are enough for the calculations of the most demanding 2D and 1D disordered structures. The absorption in the c-Si ( $A$ ) and the resulting short-circuit current density ( $J_{sc}$ ) are assumed as the main figures of merit. For the calculation of the  $J_{sc}$  and of the spectral contributions  $dJ_{sc}/dE$  we assumed a black body spectrum  $\Phi$  with  $T=5800$  K and unit internal quantum efficiency, unless specified otherwise:

$$J_{sc} = e \int \phi(E) A(E) dE = \int \frac{dJ_{sc}}{dE} dE. \quad (1)$$

The rest of the paper is organized as follows: in Sec. 2 we introduce the Lambertian limit to light trapping, while in Sec. 3 we present the results for perfectly ordered 1D and 2D photonic patterns. In Sec. 4 we move to perfectly

disordered 1D Gaussian rough surfaces. The main features for these two complementary approaches are investigated. To take advantage of both of them, we propose a 1D photonic pattern with engineered size and position disorders in Sec. 5. A quick summary of the numerical results, together with the conclusions and the future developments are given in Sec. 6.

### 2 THE LAMBERTIAN LIMIT TO LIGHT TRAPPING

We assumed the Lambertian limit to light trapping [16,17] as the ultimate goal in terms of optical design. This ideal structure is sketched in the inset of Fig. 1: the c-Si slab is corrugated at the front surface with a roughness that scatters light inside the active medium. This surface is perfectly impedance-matched to the dielectric surroundings, so no reflection occurs, and it scatters sunlight with angular distribution function (ADF) proportional to the cosine of the scattering direction  $\vartheta$ :

$$ADF_{1D} = \frac{1}{2} \cos \vartheta \quad ADF_{2D} = \frac{1}{\pi} \cos \vartheta. \quad (2)$$

The different normalization factors in Eq. (2) are due to 1D or 2D downward scattering: in the former case, light is scattered only along the x direction, while both x and y directions are allowed for the latter case. From these ideal assumptions, it is possible to derive the ultimate limit to absorption following a ray optics approach [17,19]. From absorption we calculate the photo generated current under AM 1.5 spectrum [18], which is shown in Fig. 1. As evident, the 2D scattering system is much more performing thanks to the larger contribution from diffraction. For comparison we plot also the single pass case (with zero reflection losses). It is evident that there is much room for improvement for the case of c-Si, due to its indirect band gap nature. In addition, with a proper light trapping design, in the next future it seems reasonable to reach high photo generated currents with just few microns of active material.

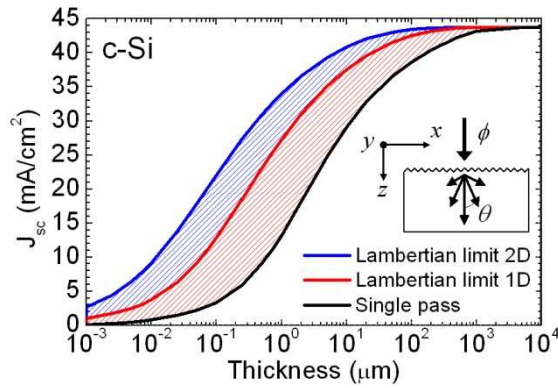


Figure 1. Short-circuit current density  $J_{sc}$  for the Lambertian limit to light trapping for the case of c-Si with 1D and 2D scattering surfaces. The optical data for c-Si are taken from Ref. [15].

## 2 ORDERED 1D AND 2D PHOTONICS STRUCTURES FOR LIGHT TRAPPING

The ordered photonic structures under investigation are sketched in Figs. 2(a)-2(c). A thin planar c-Si slab with silver back reflector (data taken from Ref. [15]) and a 70 nm thick AR coating is used as realistic reference cell (Fig. 2(a)). To trap sunlight, the front surface of the device is etched with a 1D lattice of stripes (Fig. 2(b)) or a 2D square lattice of holes (Fig. 2(c)). The same transparent material with  $n=1.65$  is used as AR coating and in the patterned layer. The total thickness is denoted with  $d$ , the pattern's period with  $a$ , and the etching depth with  $h$ . The investigated thicknesses span the border range between the Ray Optics and the Wave Optics regimes (from 0.25 to 4  $\mu\text{m}$ ), and also the typical periods are comparable with the wavelength of solar light (few hundreds of nm). In this way, interference and diffraction effects are mixed, and a good way to find out the optimal configurations for light trapping is to calculate a contour plot of the  $J_{sc}$  varying both the etching depth and the silicon fraction in the patterned layer. This is shown in Fig. 2(d) for the case of the 2D lattice with period  $a=600$  nm and total thickness  $d=1$   $\mu\text{m}$ . Different shallows and deep coupling regimes emerge for both 1D and 2D structures [4,5]. Shallow patterns are preferable from the points of view of fabrication, side-wall passivation, and internal charge transport, so we will focus on this kind of patterns. As evident, a relative increase up to +50% in the  $J_{sc}$  is achievable by proper pattern optimization. The relative increase becomes more important for thinner structures, as shown in Fig. 3. For example, the relative increase exceeds +80% for very thin cells (thickness  $d=0.25$   $\mu\text{m}$ ). This contribution, instead, is less relevant for thicker structures ( $d=2$  or 4  $\mu\text{m}$ ), where the single pass absorption can be high in most of the investigated spectral range. The contribution of diffraction can be tuned by changing the pattern's period  $a$ . The optimal pattern period is determined by the need to increase the absorption at low energy: the thinner the cell, the wider this spectral window will be. As a result, the optimal period is rather short for thin cells ( $a=500$  nm for thickness up to 0.5  $\mu\text{m}$ ), while it becomes larger for the thicker cells, where only the low energy light has to be diffracted.

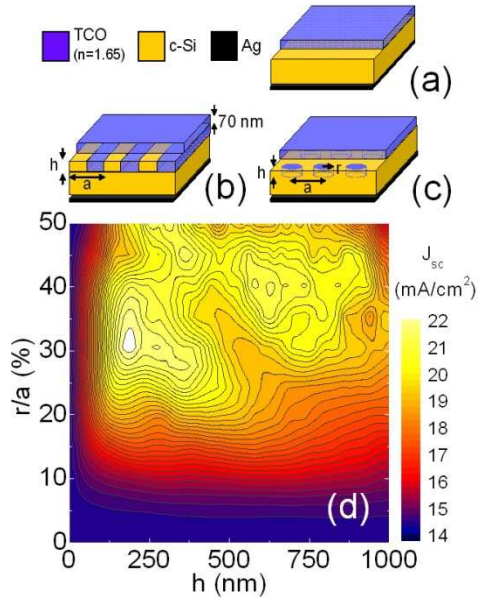


Figure 2. Sketch of the ordered photonic structures under investigation: the planar reference cell (a), the 1D pattern (b), and the 2D pattern (c). The same dielectric medium with  $n=1.65$  is used in the photonic pattern as well as AR coating (the AR thickness is 70 nm). Contour plot of the short-circuit current density  $J_{sc}$  varying the etching depth  $h$  and the ratio  $r/a$  for a 2D structure of total thickness  $d=1$   $\mu\text{m}$  and period  $a=600$  nm (d).

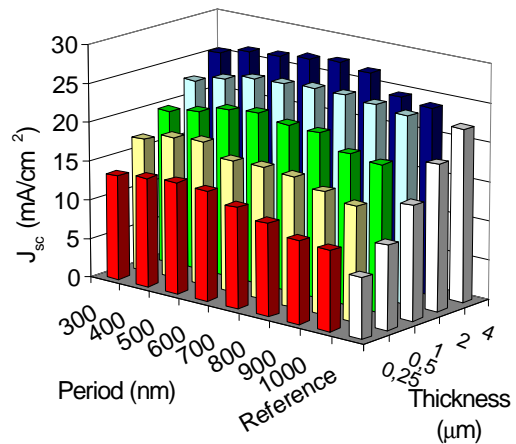


Fig. 3. Histogram of the short-circuit current density  $J_{sc}$  for 2D photonic structures for different thickness  $d$  and lattice period  $a$ .

In this way a correlation trend between the c-Si thickness and the optimal period emerges, as evident from the histogram of Fig. 3.

The main differences between patterned and planar structures are shown in terms of spectral contributions  $dJ_{sc}/dE$  to the short circuit current density in Fig. 4 for a c-Si thickness of 1  $\mu\text{m}$ . The poor absorption of the planar device below 2 eV is increased by the photonic patterns, and the 2D ones are more performing, thanks to the larger contribution from diffraction. Even if a relevant increase can be obtained, the 2D Lambertian limit is still far, and a better optical design has to be found.

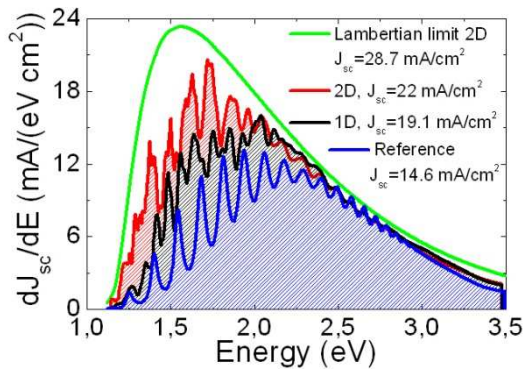


Figure 4. Spectral contributions  $dJ_{sc}/dE$  to the short-circuit current density for the reference cell (blue line), the optimized 1D (black line) and 2D (red line) patterns, and the 2D Lambertian limit (green line).

### 3 GAUSSIAN DISORDER AT RANDOMLY ROUGH INTERFACES

The investigated structure is presented in Fig. 5. It consists of 70 nm thick anti-reflection layer with refractive index  $n_{ARC} = 1.65$ , 1  $\mu\text{m}$  thick crystalline silicon slab, and a silver back reflector. Optical functions for silicon and silver were taken from Ref. [15]. The rough interface is incorporated between the silicon and AR layer, and is responsible for light trapping. Volume of the silicon is assumed to be constant.

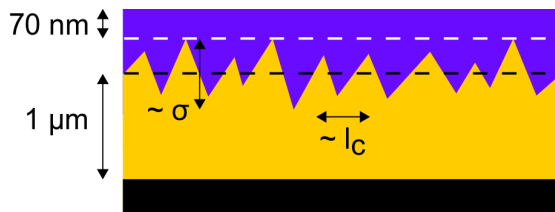


Figure 5. Structure under investigation. Rough interface is incorporated between AR layer and 1  $\mu\text{m}$  thick crystalline silicon slab. Volume of the silicon is assumed to be constant.

One-dimensional rough interface is described by two statistical parameters: the root mean square (RMS) of height  $\sigma$  and the lateral correlation length  $l_c$ . Correlation length is defined as a distance, at which normalized Gaussian correlation function decreases by  $1/e$ . Average spacing between consecutive minima/maxima of the rough interface is proportional to the lateral correlation length and is given by  $1.2837 \times l_c$  [6]. The algorithm used to generate random surface with a given statistical parameters was taken from Ref. [7]. This model of Gaussian roughness is suspected to give a good representation for rough substrates, commonly used in thin-film solar cells. Thus, presented results could be transferred to more realistic solar cell structures. As was mentioned before, absorption in the active layer is calculated by solving the set of Maxwell equations using RCWA formalism. This approach requires structures to be divided into the set of layers, periodic in the plane of the cell and homogeneous in the lateral direction – this is so-called *staircase approximation*.

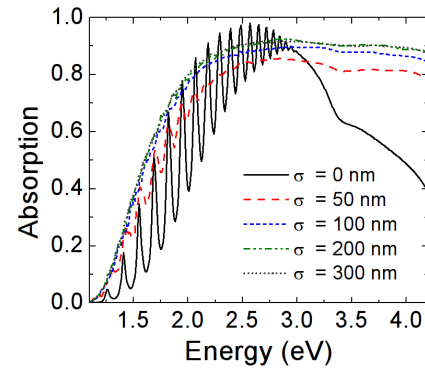


Figure 6. Absorption spectra, calculated for  $l_c = 100$  nm and different values of  $\sigma$ .

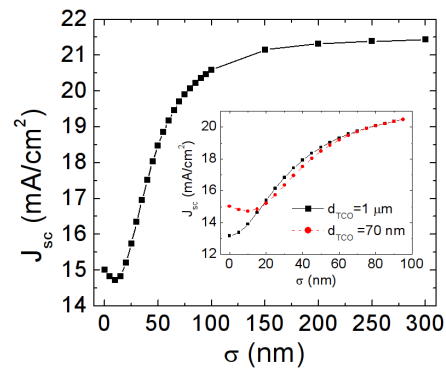


Figure 7. Short-circuit current density as a function of  $\sigma$  for  $l_c = 100$  nm. Inset presents the behavior of  $J_{sc}$  in small- $\sigma$  region in more detail.

Convergence with the number of plane waves and with the discretization of the computational area has been carefully checked. Moreover, super cell period, equal to the period of the generated random roughness, was large enough to neglect the effects of periodicity. To simulate rough interfaces, we typically use supercells between 10 and 20  $\mu\text{m}$ . As for the other simulations presented in this paper, incident solar spectrum was approximated with the black body spectrum, but this time the energy window was enlarged and the calculations were conducted for energies between 1.1 and 4.2 eV. It was done in order to fully appreciate strong antireflection action, provided by the rough interface in the high energy range. In Fig. 6 we show absorption spectra, calculated for  $l_c = 100$  nm and different values of  $\sigma$ , where the curve for  $\sigma = 0$  corresponds to the structure with flat TCO/Si interface. Absorption spectra for  $\sigma > 0$  were calculated as an average of absorption spectra for ten surface realizations with the same values of  $l_c$  and  $\sigma$ , since we aim at correlating absorption enhancement with a given set of statistical parameter, rather than with a particular surface realization. From Fig. 6 it can be clearly seen, that on increasing  $\sigma$ , Fabry-Perot oscillations are smeared out. For  $\sigma$  large enough, no sharp resonance peaks are observed, neither for an averaged spectra, nor for the absorption spectra calculated for a single realization. This is consistent with the conclusions from previous studies of disordered photonic structures [8], where no isolated diffraction peaks were observed. It suggests, that

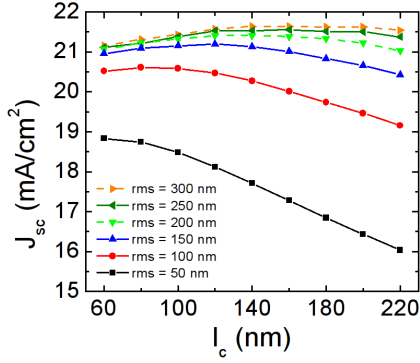


Figure 8.  $J_{sc}$  as a function of the correlation length for several different values of the root mean square of height.

the rough interface may effectively improve light trapping over a wide energy spectrum. It is different from the results obtained for an ordered light trapping structures, where significant absorption enhancement, even beyond Lambertian limit, is obtained only in a narrow energy ranges [9].

In Fig. 7 we show short-circuit current density as a function of  $\sigma$  for  $l_c=100$  nm. For  $\sigma$  larger than several tens of nm,  $J_{sc}$  increases steadily up to the saturation value of around  $21.5$  mA/cm<sup>2</sup>. This trend of the short-circuit current has been previously demonstrated for the existing, two-dimensional rough substrates [10], which suggests, that presented one-dimensional Gaussian model captures the same physical behavior as observed for a real surface topographies.

Inset in Fig. 7 presents the behavior of  $J_{sc}$  in small- $\sigma$  region in more detail. Here,  $J_{sc}$  calculated for an optimized AR layer thickness of 70 nm is compared with the values obtained for a structure with 1  $\mu$ m thick AR layer. In the former case,  $J_{sc}$  value decreases for small  $\sigma$ , which is connected to the loss of AR properties, since the effective AR layer thickness increases. In the latter case, thickness of the AR layer is far from the optimal value, thus  $J_{sc}$  for a flat TCO/Si interface is smaller, but then it increases monotonically. For large  $\sigma$ ,  $J_{sc}$  does not depend on AR layer thickness.

Finally, in Fig. 8 we show  $J_{sc}$  as a function of the correlation length for several different values of the root mean square of height. It is demonstrated, that the optimal value of  $l_c$  depends on  $\sigma$  and varies significantly, between less than 80 nm (small  $\sigma$ ) and around 160 nm (large  $\sigma$ ). Thus, taking into account this correlation between two statistical parameters describing the disorder is essential to obtain rough interfaces, giving substantial absorption enhancement.

#### 4 1D PHOTONIC STRUCTURES WITH ENGINEERED SIZE AND POSITION DISORDERS

In the previous sections we obtained good results in terms of absorption enhancements with both ordered and disordered photonic structures. The main advantage of ordered structures is the tunability of diffraction, which allows to selectively couple the incident light inside the cell by changing some controllable lattice parameters (period, etching depth, and silicon fraction). The drawback is that the resonances induced in the absorption spectra are narrow; hence a large number of them is needed to produce a relevant photocurrent enhancement [1]. On the contrary, the main advantage of disordered

structures is that the absorption can be uniformly increased and the resonances in the spectra are spread out. The drawback is that from a practical point of view it is more difficult to control the basic parameters (rms and correlation length) to obtain exactly the desired surface roughness. Our goal is to design a structure where the optimized ordered configuration is modified by introducing a controlled amount of Gaussian size and position disorders [14]. In this way the advantages of both order and disorder can be retained, with significant improvements in the optical design. To save up computational time, we limit to disordered 1D structures. The underlying physical mechanisms are the same for both the 1D and 2D cases, but calculations are much more demanding for the latter case.

The structures under investigation are shown in Figs. 9(a) and 9(b). The optimized 1D ordered configuration (whose spectrum is reported in Fig. 4 with black line) has period  $a_0=500$  nm, etching depth  $h=200$  nm and silicon fraction  $f_{Si}=70\%$  (Fig. 9(a)). A super cell with period  $a=10a_0=5$   $\mu$ m is introduced to define the disordered structures in the RCWA formalism (Fig. 9(b)). The Gaussian disorder is applied to both the position of the centres of the silicon stripes ( $x_i$ ) and to their width ( $w_i$ ) by means of displacement  $\Delta x_i$  and  $\Delta w_i$  (in our case the index  $i$  runs from 1 to 10). The displacements are Gaussian distributed with mean zero and standard deviations  $\sigma_x$  and  $\sigma_w$ :

$$P(\Delta x_i) = \frac{1}{\sqrt{2\pi}\sigma_x} e^{-\Delta x_i^2/2\sigma_x^2} \quad (3)$$

$$P(\Delta w_i) = \frac{1}{\sqrt{2\pi}\sigma_w} e^{-\Delta w_i^2/2\sigma_w^2}. \quad (4)$$

The etching depth and the silicon fraction are the same of the ordered configuration. We calculate the short-circuit current density by varying  $\sigma_x$  and  $\sigma_w$  (respecting the non-overlap condition), as shown in the contour plot of Fig. 5(c). Twenty structures with the same parameters are calculated for each value of the disorder: the  $J_{sc}$  reported in Fig. 5(c) is averaged over these configurations. As it is evident, the ordered configuration is always improved, and a complex 2D correlation scheme arises in the ( $\sigma_x, \sigma_w$ ) plane. The maximum is located at  $\sigma_x=50$  nm and  $\sigma_w=25$  nm, along the  $\sigma_w/\sigma_x=2$  direction. This trend is used to investigate the Gaussian disorder with just one parameter  $\sigma_a$ , which is related to the pure size and position disorders by:

$$\sigma_w = f_{Si}\sigma_a \quad \sigma_x = f_{Si}\sigma_a/2. \quad (5)$$

Fifty structures with the same  $\sigma_a$  are investigated, with  $\sigma_a$  in the range from 0 to 150 nm. The optimal configuration is found at  $\sigma_a=50$  nm, and the spectral contributions  $dJ_{sc}/dE$  of the best structure are shown in Fig. 10. As evident, the spectral response is increased over the whole spectral range, with a broadening of the resonances. In terms of  $J_{sc}$ , we obtain  $20.85$  mA/cm<sup>2</sup> with the best disordered structure, a value remarkably close to the 1D Lambertian limit to light trapping at  $22.7$  mA/cm<sup>2</sup>. The general features of the plot of Fig. 9(c) and of the optical spectra can be understood from the Fourier analysis of the periodic dielectric function of the patterned layer, together with basic considerations about the guided modes supported by the structures.

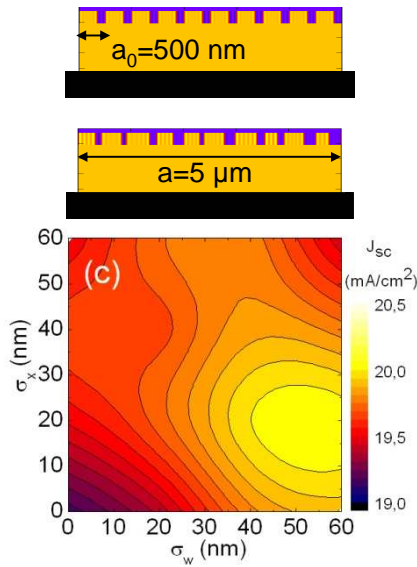


Figure 9. Edge view of the solar cells with the ordered photonic configuration (a), and with Gaussian size and position disorder  $\sigma_w=60$  nm,  $\sigma_x=60$  nm (b). Contour plot of the  $J_{sc}$  averaged over 20 structures with given  $\sigma_w$  and  $\sigma_x$  (c).

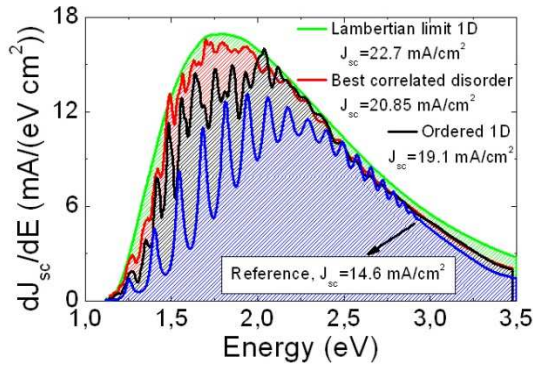


Figure 10. Spectral contributions  $dJ_{sc}/dE$  to the short circuit current for the reference planar cell (blue line), for the optimized 1D ordered configuration (black line), for the optimized disordered configuration with  $\sigma_a=50$  nm (red line), and for the 1D Lambertian limit (green line).

A schematic plot of the TE guided modes (electric field along the  $y$  direction) of a  $1 \mu\text{m}$  thick c-Si slab in air is reported in Fig. 11(a). The amplitudes of the Fourier coefficients of the dielectric function  $|\epsilon(k_{//})|$  governs the diffraction process [3,14]. A larger coefficient  $\epsilon(k_{//})$  means larger coupling of light to the guided modes, if the proper phase-matching condition is satisfied. This is drawn with black dots in Fig. 11(a), for the case of  $k_{//}=10 \times 2\pi/a$  at normal incidence. The richer Fourier spectrum of disordered structures is responsible for the increased light coupling with respect to the order configuration, where only two diffraction orders can be used. The evolution of the Fourier coefficients with the disorder level is shown in Fig. 11(b), while the comparison between pure size and position disorder is shown in Fig. 11(c). Since with a  $1 \mu\text{m}$  thick c-Si slab, the absorption has to be increased below 2 eV (yellow background in Fig. 11(a)), the diffraction contributions by the orders between  $|k_{//}|=10$  and  $20 \times 2\pi/a$  have to be enhanced.

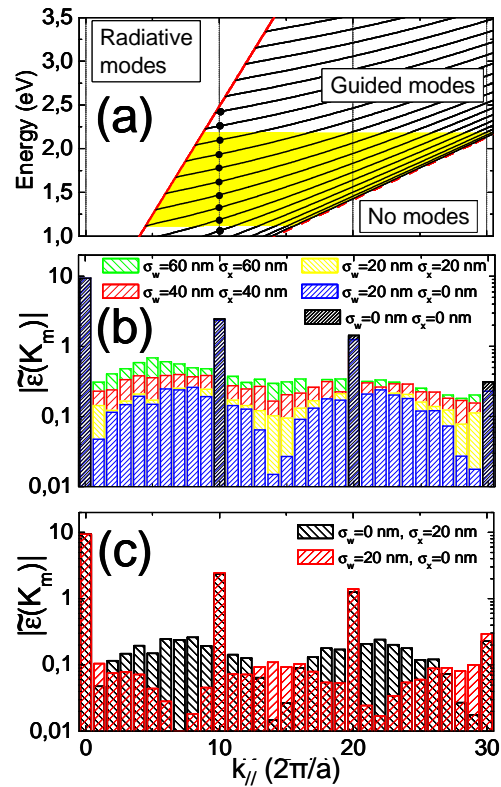


Figure 11. Dispersion of the guided modes of a  $1 \mu\text{m}$  thick c-Si planar slab in air for TE polarization (a). The spectral range for light trapping is highlighted with yellow background, and the coupling events mediated by the  $k_{//}=10 \times 2\pi/a$  reciprocal vector at normal incidence are marked with black dots. Amplitudes of the Fourier coefficients  $|\epsilon(k_{//})|$  for the dielectric function of ordered and disordered patterns (b). The same plot showing the difference between size and position disorders in terms of Fourier spectra (c).

To this end, the size disorder has a better Fourier spectrum with respect to position disorder (Fig. 11(c)). Engineering the disorder it is possible to define a structure with the desired Fourier spectrum that fits well with the selected energy window for light trapping. If the disorder becomes too large, also diffraction in air tends to be enhanced, and the  $J_{sc}$  decreases. This suggests that only a relatively small amount of disorder has to be added for best performances. These results confirm that an engineered combination of order and disorder is the optimal strategy for high-efficiency light trapping design.

## 6 CONCLUSIONS AND DEVELOPMENTS

Different types of photonic light trapping approaches for thin film c-Si solar cells have been investigated and optimized. We focused on thicknesses comparable with those of epitaxy-free fabrication techniques for c-Si, and we found that the absorption and resulting  $J_{sc}$  are remarkably increased. Such engineered optical designs could lead to very thin devices whose energy conversion efficiency may be comparable to those of well-established bulk c-Si technology. As global summary of our results, we report the  $J_{sc}$  and the relative increases that are obtained with a c-Si thickness of  $1 \mu\text{m}$  in Tab. 1.

	$J_{sc}$ (mA/cm <sup>2</sup> )	Relative increase
Reference planar	14.6	-
Ordered 1D	19.1	+31%
Roughness 1D	20.57	+41%
Gaussian disorder 1D	20.85	+43%
Lambertian limit 1D	22.7	
Ordered 2D	22	+51%
Lambertian limit 2D	28.7	

Table 1. Short-circuit current density  $J_{sc}$  and relative increase with respect to the planar reference case for different photonic solar cells obtained from a c-Si slab of thickness 1  $\mu\text{m}$ .

Relevant improvements are obtained with both ordered and disordered structures. The former take advantage of the tunability of the lattice parameters, which allows the system to be engineered depending on the specific device requirements. The latter structures have a richer Fourier spectrum, which allows a better coupling of light into the solar cell. The main advantages of these two complementary approaches have been used to design an high-efficiency light trapping structure, which is obtained starting from an optimized 1D ordered structure and introducing a controlled amount of Gaussian size and position disorders. The resulting configuration has higher absorption, and in terms of  $J_{sc}$  is very close to the 1D Lambertian limit. The main features of the optical spectra can be understood from a basic Fourier analysis of the dielectric function of the patterned layer. This result, together with the others for pure ordered and disordered structures, will be useful for the future developments, where more complex 2D photonic structures will be investigated, due to their larger potential for light trapping.

## 7 ACKNOWLEDGEMENTS

This work was supported by EU through Marie Curie Action FP7-PEOPLE-2010-ITN project no. 264687 "PROPHET" and by Fondazione Cariplo under project 2010-0523 "Nanophotonics for thin film photovoltaics".

## 8 REFERENCES

- [1] Z. Yu, A. Raman and S. Fan, "Fundamental limit of nanophotonic light trapping in solar cells", Proc. Nat. Ac. Sci. **107**(41), pp. 17491-17496 (2010).
- [2] X. Meng, E. Drouard, G. Gomard, R. Peretti, A. Fave, and C. Seassal, "Combined front and back diffraction gratings for broad band light trapping in thin film solar cell", Optics Express; **20**(S5), pp. A560-A571 (2012).
- [3] E. R. Martins, J. Li, Y. Liu, J. Zhou, and T. F. Krauss, "Engineering gratings for light trapping in photovoltaics: The supercell concept", Phys. Rev. B **86**(4), 041404(R) (2012).
- [4] S. Zanotto, M. Liscidini, and L. C. Andreani, "Light trapping regimes in thin-film silicon solar cells with a photonic pattern", Optics Express **18**(5), pp. 4260-4274 (2010).
- [5] A. Bozzola, M. Liscidini, and L. C. Andreani, "Photonic light-trapping versus Lambertian limit in thin film silicon solar cells with 1D and 2D periodic patterns",

- Optics Express **20**(S2), pp. A224-A244 (2012).
- [6] A. A. Maradudin, and T. Michel, "The transverse correlation length for randomly rough surfaces," Journal of Statistical Physics **58**, pp. 485–501 (1990).
- [7] V. Freilikher, E. Kanziiper, and A. Maradudin, "Coherent scattering enhancement in systems bounded by rough surfaces," Physics Reports **288**, pp. 127 – 204 (1997).
- [8] C. Battaglia, C.-M. Hsu, K. Soderstrom, J. Escarre, F.-J. Haug, M. Charriere, M. Boccard, M. Despeisse, D. T. L. Alexander, M. Cantoni, Y. Cui, and C. Ballif, "Light trapping in solar cells: Can periodic beat random?" ACS Nano **6**, pp. 2790–2797 (2012).
- [9] Z. Yu, A. Raman, and S. Fan, "Fundamental limit of light trapping in grating structures," Opt. Express **18**, pp. A366–A380 (2010).
- [10] C. Rockstuhl, S. Fahr, K. Bittkau, T. Beckers, R. Carius, F.-J. Haug, T. Soderstrom, C. Ballif, and F. Lederer, "Comparison and optimization of randomly textured surfaces in thin-film solar cells," Opt. Express **18**, pp. A335–A341 (2010).
- [11] V. Depauw, Y. Qiu, K. Van Nieuwenhuysen, I. Gordon, and J. Poortmans, "Epitaxy-free monocrystalline silicon thin film: first steps beyond proof-of-concept solar cells", Progr. Photovolt: Res. Appl. **19**(7), pp. 844-850 (2010).
- [12] C. Trompoukis, O. El Daif, V. Depauw, I. Gordon, and J. Poortmans, "Photonic assisted light trapping integrated in ultrathin crystalline silicon solar cells by nanoimprint lithography", Appl. Phys. Lett. **101**, 103901 (2012).
- [13] D. M. Whittaker and I. S. Culshaw, "Scattering-matrix treatment of patterned multilayer photonic structures", Phys. Rev. B **60**(4), pp. 2610-2618 (1999).
- [14] M. Liscidini, D. Gerace, L. C. Andreani, and J. E. Sipe, "Scattering-matrix analysis of periodically patterned multilayers with asymmetric unit cells and birefringent media", Phys. Rev. B **77**(3), 035324 (2008).
- [15] E. D. Palik, Handbook of Optical Constants of Solids. Academic: Orlando (1985).
- [16] E. Yablonovitch, "Statistical ray optics", J. Opt. Soc. Am. **72**(7), pp. 899-907 (1982).
- [17] M. A. Green, "Lambertian light trapping in textured solar cells and light-emitting diodes: analytical solutions", Progr. Photovolt: Res. Appl. **10**(4), pp. 235-241 (2002).
- [18] AM1.5 solar spectrum irradiance data: <http://rredc.nrel.gov/solar/spectra/am1.5>.
- [19] A. Bozzola, M. Liscidini, and L.C. Andreani, submitted (2012).